Contents

List of Figures

List of Tables

Chapter 1

Spectral Distribution of SiV centers in Nanodiamonds

In this chapter we report on our results regarding luminescence properties of SiV centers. The samples used in our investigation consists of a large set of CVD nanodiamonds containing *in-situ* SiV centers of a size in the range of 70 nm to 100 nm. Throughout the chapter we refer to samples using their distinct sample-id as listed in **??**.

The obtained fluorescence spectra of SiV centers show that both the center wavelength of the ZPL as well as the linewidth of the zero-phonon-line vary strongly among different samples. Our measurements over a large set of SiV centers indicate a strong correlation between the center wavelength of the zero-phonon-line and the corresponding linewidths, resulting in a previously unreported bimodal distribution. We assert single photon emission from these SiV centers across the whole range of zero-phonon-line positions and linewidths. Furthermore we detect fluorescence intermittency, i.e. blinking. The obtained data for the bright and dark times indicate an exponantial decay of the dark state and a log-normal decay of the bright state, the latter of which has to our knowledge not been reported as of yet.

1.1 Photoluminescence spectra

To identify nanodiamonds containing SiV centers, we performed confocal scans of the samples. To reduce bias in the measurements, not only the brightest spots of the confocal scans are investigated, but also those which barely exceed background fluorescence. SiV centers are further investigated by measuring photoluminescence (PL) spectra, single photon statistics and photostability. As discussed in **??**, the typical luminescence spectrum of an SiV center is composed of a prominent zero-phonon-line peak and weak sidebands. Investigations of both are reported independently in the following paragraphs.

1.1.1 Zero-phonon-line

The center wavelength and the linewidth of the zero-phonon-line (ZPL) of SiV luminescence spectra for samples insitu50, insitu70, and insitu100 are determined by fitting a Lorentzian

fit to the ZPL. Both spectra from single and multiple SiV centers are taken into account. In Figure 1.1 the linewidth for each measured ZPL is plotted against its center wavelength.

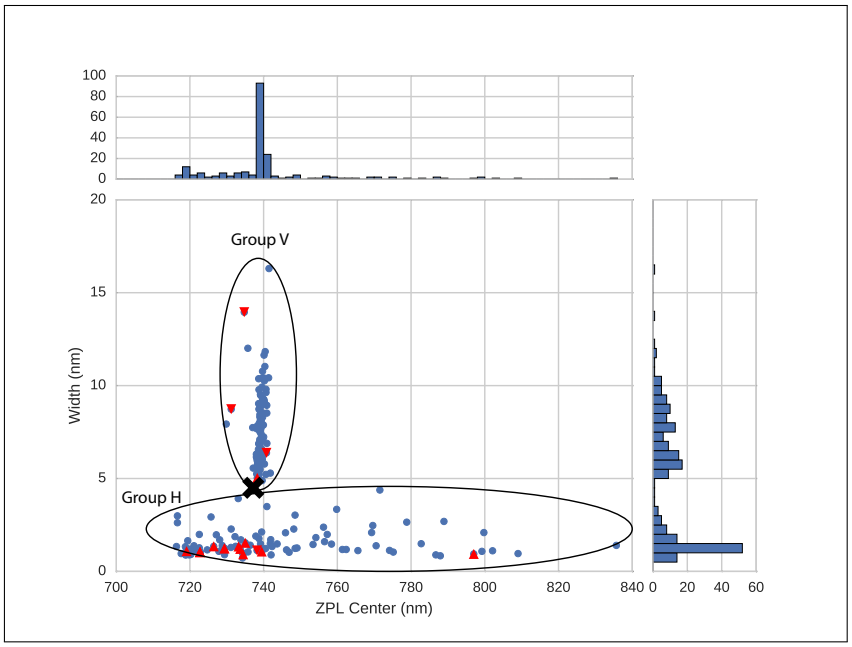

Figure 1.1: Distribution of the ZPL center wavelength versus the linewidth of the ZPL of the investigated SiV centers in milled nanodiamonds containing *in-situ* incorporated SiV centers for samples insitu50, insitu70, insitu100. The data seperates into a horizontal (group H) and a vertical (group V) cluster. The bold black cross marks the position of an ideal SiV center in unstrained bulk diamond [**?**]. The red triangles indicate emitters with an antibunching dip in the $g^{(2)}(0)$ measurement. Upwards pointing triangles represent blinking emitters (fluorescence intermittency), while triangles pointing down represent non-blinking emitters (see **??**).

What immediately strikes the eye is a pattern that to our knowledge has not been reported to date: The observed ZPLs partition into two groups, dentote a horizontal lobe (group H) and a vertical lobe (group V). The two lobes are seperated by a gap, i.e. a region with a pronouced lack of data points. Single emitters are identified both in group H and group V, marked as red triangles in Figure 1.1. Further details on single emmiters are given in section **??**.
The two groups are defined by their characteristic center wavelengths and linewidths: In group H very prominent ZPL peaks are found showing linewidths in the range of 1 nm to 5 nm and center wavelengths in the range of 715 nm to 835 nm. Figure 1.2a shows a representative spectrum of a single emitter in group H (denoted emitter H1), exhibiting a ZPL line width of 1.4 nm and a center wavelength of 726.5 nm. In contrast, in group V, the spectra exhibit broader ZPL linewidths of approximately 5 nm up to 18 nm. Their ZPL center wavelengths, however, are distributed within the very narrow range of 738 nm to 741 nm. Figure 1.2b shows a spectrum of a single emitter of group V (denoted emitter V1) with a ZPL linewidth of 6.4 nm and a center wavelength of 740.8 nm. For comparison, the room temperature ZPL of SiV centers in unstrained bulk diamond exhibits a linewidth of 4 nm to 5 nm and a center wavelength of 737.2 nm marked with a black cross in Figure 1.1 [**?**, **?**].

To determine how much the ZPLs contribute to the total observed emmision of emitter H1 and emitter V1, we determine the Debye-Waller factors for both. The Debye-Waller factor

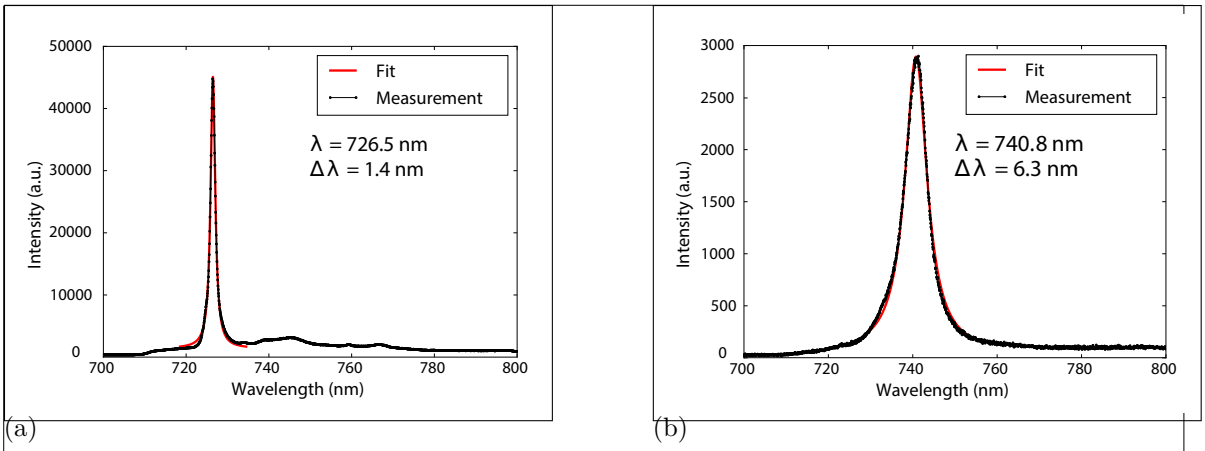

(a) (b)

Figure 1.2: Representative photoluminescence spectra of sample insitu100ao measured at room temperature. (a) Spectrum of group H of Figure 1.1, denoted emitter H1. (b) Spectrum of group V of Figure 1.1, dentoted emitter V1. The red lines are Lorentzian fits to the peaks.

is defined by $DW = I_{ZPL}/I_{TOT}$ and is therefore suited as a measure for sideband intensity. The Debye-Waller factor for emitter H1 amounts to 0.81 ± 0.01 (given uncertainty due to fit). This Debye-Waller factor corresponds to a Huang-Rhys factor $S = -\ln(DW)$ [**?**] of 0.21 ± 0.01, which is in good agreement with the values reported in [**?**]. The error is mainly due to background corrections. When zooming in onto the spectrum of emitter V1 we do not find distinct sidebands peaks, i.e. almost all emission for this emmiter is alloted to the ZPL. Considering resolution limits of the spectrometer, darkcounts and fluorescence background, we evaluate the Debye-Waller factor to be larger than 0.97. It is the largest Debye-Waller factor amongst all our milled SiV centers. The two mentioned Debye-Waller factors should not be interpreted as single representative emitters for the respective groups, they rather serve as an orientation of the spread of the Debye-Waller factors of both groups. It has to be pointed out, that we did not find any systematic difference of the Debye-Waller factor between group H and group V.
To provide context for the novel findings presented in Figure 1.1, we compare our results to various earlier findings. Furthermore, we discuss an additional comparison to an investigated control sample fabricated using silicon implantation. The resuls are presented in Figure 1.3.

Samples for which previous data has been taken are:

1. nanodiamonds produced by bead-assisted sonic disintegration (BASD) of polycrystalline CVD diamond films (blue rings in Figure 1.3 [**?**]; data taken from [**?**])
2. nanodiamonds produced directly via a CVD process with *in-situ* incorporated SiV centers; measured in a spectral filter window of 730 nm to 750 nm (blue squares in Figure 1.3; data reused from [**?**] with permission)
3. nanodiamonds produced in the same manner as the CVD sample in 2 (blue downwards pointing triangles in Figure 1.3; produced by M. Schreck [**?**]; spectroscopic measurement performed with setup described in **??**)

All previous data from different nanodiamond material fit nicely with the ZPL distribution presented in Figure 1.3, confirming the findings of Figure 1.1.
We verify that the observed luminescent defects are indeed silicon related by performing con-

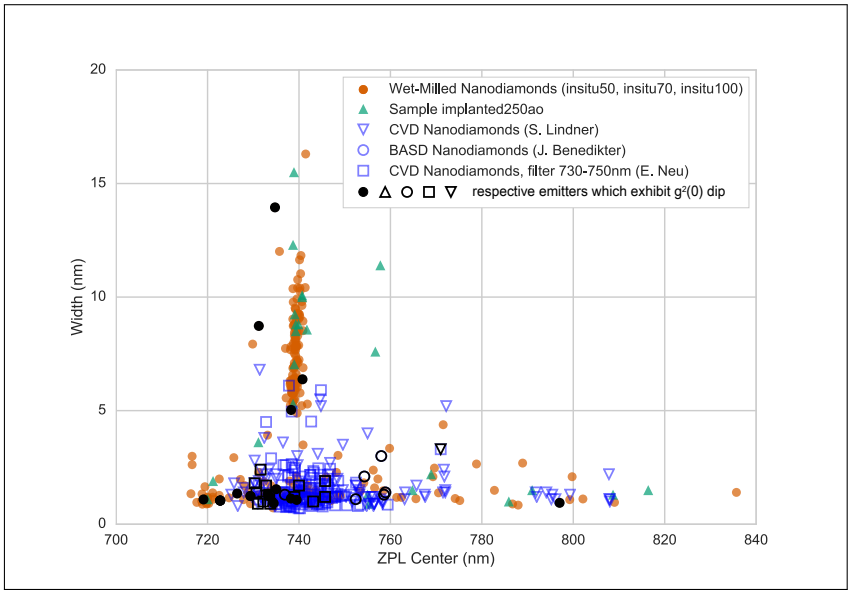

Figure 1.3: Comparison of the distribution of the linewidth vs. the center wavelength of the ZPL of the investigated SiV centers in milled nanodiamonds (samples insitu50, insitu70, insitu100) with data measured on sample implanted250ao (implanted with Silicon); with data measured in our group on CVD nanodiamonds produced by M. Schreck [**?**]; with data measured on nanodiamonds reported by J. Benedikter in [**?**]; and with data measured in CVD diamonds by E. Neu in a filter window between 730 nm and 750 nm [**?**]. Black symbols represent emitters exhibiting a dip in the $g^{(2)}(0)$ function, indicating a single or very few SiV centers

trol experiments with silicon implanted samples (sample implanted250ao). By doing so we rule out the possibility that the two lobes in the distribution are a result of artifacts. Such artifacts include other elements incorporated into the nanodiamonds during the growth process: Residue from previous processes performed in the diamond growth chamber or material from chamber parts may be incorporated during nanodiamond growth. Figure 1.3 shows that the implanted SiV centers cover roughly the same spectral range as the *in-situ* incorporated centers from around 720 nm to 820 nm as the *in-situ* incorporated centers. This correlation provides strong evidence for the silicon related origin of the defects.
To provide a theoretical interpretation, the ZPL center wavelength shift is investigated in further detail and compared to results from density functional calculations. Zooming in to group V (Figure 1.4a) it becomes clear that only six of the measured data points in group V are situated at a shorter center wavelength than the point attributed to an ideal SiV center in unstrained bulk material. The the shortest wavelength shift is at 729.9 nm. At the same time, much more data exhibit a center wavelength bigger than the ideal SiV center. This asymmetry suggests that a red-shift of the ZPL of an SiV center is significantly more likely than a blueshift.

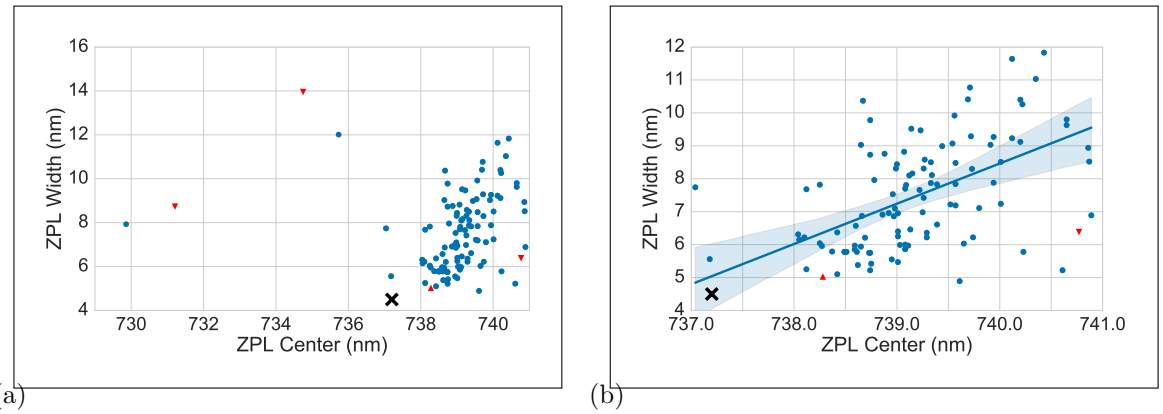

(a) (b)

Figure 1.4: (a) A zoom into group V. While many data points exhigit higher center wavelengths (i.e. a redshift) than the ideal SiV center in bulk, only few exhibit shorter center wavelengths (i.e. a blueshift). (b) Zooming further into group V, a clear trend of broader ZPL linewidths for larger ZPL center shifts is visible. The line in a linear regression to all datapoints between 737 nm and 741 nm which exhibit a linewidth bigger than 4 nm.

Several mechanisms contribute to the center wavelength shift, predominantely hydrostatic- and material strain. As explained in **??**, we measured the Raman shift of samples insitu70 and implanted250ao. These measurements indicate strain in the diamond lattice in the range of -8.56 GPa to 4.26 GPa. Figure 1.5 shows results from density funtional calculations. The shift of the ZPL is modelled in dependence of pressure in the diamond lattice both for hydrostatic stress and for uniaxial stress. Figure 1.5 illustrates that the assumption stated in **??**, namely that the strain in the nanodiamonds is due to hydrostatic and uniaxial stress, corresponds well with the measured ZPL shifts in group V.

With higher uniaxial pressure, the ZPL becomes more and more red-shifted. The blueshifted ZPL center wavelengths are explained by hydrostatic stress in the diamond material. The strain calculated from the Raman measurements corresponds well with the results in Figure 1.5 for group V. However, the measured shifts in group H are too broad to be solely explained by strain in the diamond. A potential explanation for the very broad distribution of defect

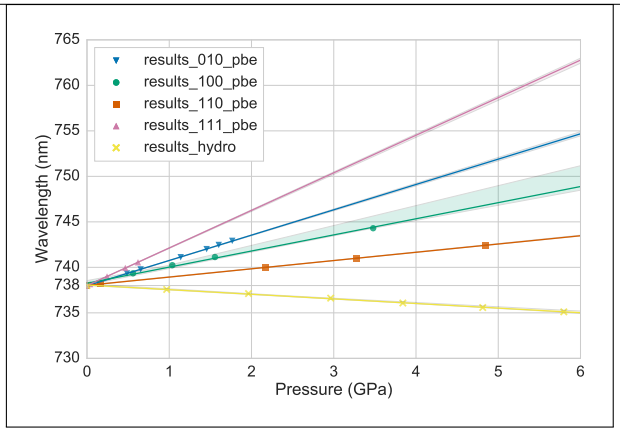

Figure 1.5: Calculations of the wavelength of the SiV center ZPL in dependence of pressure. Markers: calculated pressure with PBE functional; Lines: linear fits to the calculated points, the shaded area around the lines representing the one sigma (68%) confidence intervall. Yellow: hydrostatic pressure; other colors: uniaxial pressure, for different orientations. All calculations are performed with a PBE functional. Hydrostatic-type pressure causes a moderate blue shift whereas uniaxial strain causes larger redshift with different magnitudes depending on the direction of the strain

center ZPL center wavelengths could be the association of SiV centers with a further nearby defect, such as a vacancy, or a modified SiV complex such as SiV:H [**?**].
Zooming in to group V, another effect becomes visible (Figure 1.4b): With increasing ZPL center wavelength, the linewidth becomes broader. As discussed above, a red-shift of the ZPL is linked to increasing uniaxial strain. Thus we conclude that the ZPL linewidth too is affected by strain in the diamond lattice. Here, a modified electron-phonon coupling [**?**] causes increased uniaxial stress, resulting in larger linewidths. A similar effect has been previously observed for SiV centers at cryogenic temperatures [**?**].
To conclude, we are able to explain the distribution of ZPL center wavelengths in group V very consistently with theoretical predictions based on perturbative shifts due to strain in the diamond lattice. On the other hand, we have to assume that group H is comprised of modified SiV centers, the structure of which is currently unclear.